The essential work of fracture and JR curves for the double cantilever beam specimen : an examination of elastoplastic crack propagation

Atkins, A. G.; Chen, Zhong; Cotterell, Brian

1998

Atkins, A. G., Chen, Z., & Cotterell, B. (1998). The Essential Work of Fracture and JR Curves for the Double Cantilever Beam Specimen: An Examination of Elastoplastic Crack Propagation. Proceedings of The Royal Society of London A, 454(1971), 815-833.

https://hdl.handle.net/10356/95332

https://doi.org/10.1098/rspa.1998.0187

The essential work of fracture and J_R curves for the double cantilever beam specimen: an examination of elastoplastic crack propagation

By A. G. Atkins[1], Z. Chen[1] and B. Cotterell[2]

[1]*Department of Engineering, University of Reading, PO Box 225, Whiteknights, Reading RG6 6AY, UK*

[2]*Institute of Materials Research and Engineering, National University of Singapore, Singapore 119260, Republic of Singapore*

The propagation of a crack in a double-cantilever beam (DCB) geometry where there is extensive remote plastic flow both preceding and accompanying fracture is analysed. Experiments show that there is an appreciable path dependence in load–deflection-crack length behaviour because of the remote residual plastic zones left in the wake of the crack front. The deflection for a propagated crack is greater than the deflection predicted by nonlinear fracture mechanics since in real plasticity the plastic deformations cannot be recovered and their 'energy' released back into the system. A Griffith energy approach is employed to uncouple the work increments of elastic strain energy, the remote plastic work and the essential crack-tip fracture work. For geometries other than the DCB these components cannot be easily uncoupled. Analyses are given for elastic perfectly plastic solids and for elastic power-law work-hardening materials. There is good agreement with experiments on side-grooved double cantilever beam specimens made from 6082-TF aluminium alloy (which is almost elastic perfectly plastic) and from annealed α-brass (which work hardens appreciably). Varying degrees of elastoplasticity during propagation are obtained by altering the height of the beam arms; globally elastic fracture results are obtained with adequately deep arms.

It is found that the load–deflection curves can be predicted by assuming the essential work of fracture at the crack tip is constant, at initiation and propagation, for both these materials. In contrast the J_R curves calculated from the load–deflection diagram by the conventional method are dependent on the specimen size because they contain non-recoverable global plastic work.

Keywords: elastoplastic fracture mechanics; fracture; ductile fracture; crack resistance curves; J_R curves; DCB testpiece

1. Introduction

The load and displacement at fracture initiation, in a body undergoing extensive irreversible plastic flow prior to cracking, can be predicted using a deformation theory of plasticity which is the same as assuming that the material is reversibly nonlinear

elastic (NLE) (Kachanov 1971). Because of this equivalence, it is possible to use NLE theories for the initiation of ductile fracture. In particular the J integral at initiation gives the essential work of fracture, R, in the fracture process zone (FPZ) at the crack tip (Rice 1968)

$$R = \int_0^{\delta_f} \sigma \, \mathrm{d}\delta, \tag{1.1}$$

where σ is the stress in the FPZ, δ is the crack-opening displacement across the FPZ and δ_f is the crack opening at which the fracture becomes complete. The J-integral can also be obtained from the rate change in the NLE potential energy, Π, with fracture area A, at initiation†,

$$R = J = -\frac{\mathrm{d}\Pi}{\mathrm{d}A} = -\left[\frac{\partial \Lambda}{\partial A}\right]_u = \left[\frac{\partial \Omega}{\partial A}\right]_P, \tag{1.2}$$

where Λ and Ω are the NLE strain and complementary energy, respectively, P is the external load and u is the load-line deflection. In an elastoplastic solid, stress and strain ratios at a point are nearly constant before fracture initiation and are exactly constant for the special case of the double cantilever beam (DCB) specimen. Hence an effective nonlinear strain energy, Λ, can be identified by

$$\Lambda = \Lambda_e + \Gamma_p, \tag{1.3}$$

where Λ_e is the elastic strain energy and Γ_p is the plastic work.

The J-integral has been extended by many authors to cover crack growth. There are obvious difficulties in extending an NLE theory to elastoplastic (ELP) crack propagation where near the tip of the crack elastic unloading causes the stress and strain ratios to change radically. It was argued by Hutchinson & Paris (1979) that crack growth would be J-controlled for limited crack extensions and that under these conditions the J_R crack growth resistance curves would be dependent only on the crack extension. However, unless the plastic zone is well contained within an elastic stress field, J_R is independent of size and geometry only for small crack extensions (Hancock *et al.* 1993; Joyce & Link 1995; Xia *et al.* 1995: Xia & Shih 1995).

J_R curves are generally size and geometry dependent because the energetic interpretation of J includes the work in the plastic zone as well as the work in the FPZ (Cotterell & Atkins 1996). In the work-rate equation for elastoplastic crack propagation (Havner & Glassco 1966), the work rate of the external forces $\mathrm{d}W/\mathrm{d}A$ is given by

$$\frac{\mathrm{d}W}{\mathrm{d}A} = P\frac{\mathrm{d}u}{\mathrm{d}A} = \frac{\mathrm{d}\Lambda_e}{\mathrm{d}A} + \frac{\mathrm{d}\Gamma_p}{\mathrm{d}A} + R. \tag{1.4}$$

Equation (1.4) without Γ_p is, of course, the displacement-reversible elastic fracture mechanics' relation used by Griffith (1921) in his seminal study. There is no *a priori* assumption that R is constant in equation (1.4). The FPZ can be identified with the region of strain softening that causes localization of the deformation into a narrow zone. Within the FPZ voids nucleate and grow causing strain softening. The deformation within the FPZ can be modelled by constitutive equations that take account

† The equivalence between J and the potential energy release rate is strictly true only if Barenblatt's (1962) two hypotheses of a small FPZ and steady-state propagation with no change in the shape of the FPZ are valid. However, though in theory J is not exactly given by equation (1.1) the difference in practice is usually negligible (Cotterell & Atkins 1996).

of the effect of the growing voids on the macroscopic stress and which, unlike plastic deformation of solid materials, is sensitive to the hydrostatic stress. A variety of constitutive equations has been proposed which are basically very similar; the most popular is the Gurson model (1977) as modified by Tvergaard (1982). There is an interactive relationship between the deformation within the FPZ and the surrounding plastic zone. Within the FPZ there is void growth and its compliance is much greater than that in the surrounding plastic zone; as a consequence under plane strain conditions the FPZ deforms nearly uniaxially with an increase in volume. The effect of variation in constraint caused by different specimen geometries is, therefore, most likely to be felt in the surrounding plastic zone rather than in the FPZ itself.

In this paper a very particular geometry, the deep side-grooved double-cantilever beam (DCB) specimen, is considered. In this geometry, if the tip is loaded by a moment, the crack propagation is steady-state and R must be constant (Cotterell *et al.* 1996). Such behaviour is unusual and in all other geometries, unless the plastic zone is small compared with the crack length, crack growth is far from steady-state. Thus, the deep side-grooved DCB specimen is very suited to studying spurious crack growth resistance. For a force-loaded DCB specimen, provided that the length to height ratio is reasonably large, the crack propagation will be practically steady-state from initiation and the variation in the specific work of fracture, R, is negligible. In general the terms in equation (1.4) depend upon the crack-propagation history and are not easily separable. There are two unique properties of the DCB specimen. If the load increases then there is no unloading anywhere. On the other hand, if the end load is constant or decreases, plastic deformation occurs only ahead of the crack tip. No other geometries have these properties. Therefore if the load rises, ELP behaviour is identical to NLE and equation (1.2) applies to propagation as well as initiation. The case of crack propagation under falling end load in a real ELP material needs to be considered in more detail. Equation (1.4) can be written in terms of the partial derivatives

$$\frac{\mathrm{d}W}{\mathrm{d}A} = P\left\{\left[\frac{\partial u}{\partial P}\right]_A \frac{\mathrm{d}P}{\mathrm{d}A} + \left[\frac{\partial u}{\partial A}\right]_P\right\} = \left[\frac{\partial}{\partial P}(\Lambda_\mathrm{e} + \Gamma_\mathrm{p})\right]_A \frac{\mathrm{d}P}{\mathrm{d}A} + \left[\frac{\partial}{\partial A}(\Lambda_\mathrm{e} + \Gamma_\mathrm{p})\right]_P + R, \tag{1.5}$$

where, because there is no plastic deformation behind the crack tip under falling load,

$$\left[\frac{\partial \Gamma_\mathrm{p}}{\partial P}\right]_A = 0 \tag{1.6}$$

and the virtual work theorem gives

$$P\left[\frac{\partial u}{\partial P}\right]_A = \left[\frac{\partial \Lambda_\mathrm{e}}{\partial P}\right]_A. \tag{1.7}$$

Hence

$$R = P\left[\frac{\partial u}{\partial A}\right]_P - \left[\frac{\partial}{\partial A}(\Lambda_\mathrm{e} + \Gamma_\mathrm{p})\right]_P = \left[\frac{\partial \Omega}{\partial A}\right]_P. \tag{1.8}$$

The effective strain energy for an ELP material is $\Gamma_\mathrm{e} + \Lambda_\mathrm{p}$ ahead of the crack tip and Γ_e behind the crack tip where there is no plastic work during crack propagation. Note that during propagation the effective complementary strain energy, Ω, for an ELP material cannot be obtained directly from the load-deflection diagram.

Alternatively u and A can be chosen as the independent variables and equa-

tion (1.4) can be written as

$$\frac{\mathrm{d}W}{\mathrm{d}A} = P\frac{\mathrm{d}u}{\mathrm{d}A} = \left[\frac{\partial}{\partial u}(\Lambda_\mathrm{e} + \Gamma_\mathrm{p})\right]_A \frac{\mathrm{d}u}{\mathrm{d}A} + \left[\frac{\partial}{\partial A}(\Lambda_\mathrm{e} + \Gamma_\mathrm{p})\right]_u + R, \tag{1.9}$$

where, since in ELP the plastic work term, Γ_p, is not simply a function of u and A but depends upon whether an element is loading or unloading, the crack must be imagined to propagate at constant deflection u and then for the deflection to increase to its new equilibrium value at constant crack length. There is no plastic work except at the crack tip if the incremental crack growth takes place in this order, as is the case during natural crack growth, and

$$\left[\frac{\partial \Gamma_\mathrm{p}}{\partial u}\right]_A = 0. \tag{1.10}$$

By Castigliano's theorem

$$P = \left[\frac{\partial \Lambda_\mathrm{e}}{\partial u}\right]_A. \tag{1.11}$$

Hence

$$R = -\left[\frac{\partial}{\partial A}(\Lambda_\mathrm{e} + \Gamma_\mathrm{p})\right]_u = -\left[\frac{\partial \Lambda}{\partial A}\right]_u, \tag{1.12}$$

where the effective strain energy for an ELP material is $\Lambda_\mathrm{e} + \Gamma_\mathrm{p}$ ahead of the crack tip and Λ_e behind the crack tip and the effective strain energy, Λ, cannot be obtained directly from the load–deflection diagram. Therefore, for the special case of the DCB specimen, equations (1.8) and (1.12) are identical to equation (1.2) provided that the partial derivatives of Λ and Ω are properly calculated. Thus the essential work of fracture, R, and by definition, J, are given by equation (1.2) during propagation as well as initiation. At initiation there is no distinction between NLE and ELP behaviour for the DCB specimen since there is no unloading. There is little distinction for other geometries too at initiation and both Λ and Ω can be obtained from a load–deflection diagram. However, during crack propagation in the DCB specimen, the effective strain and complementary strain energies, that must be used in order that equation (1.2) gives the correct value of J and R, must reflect the true ELP behaviour where unloading takes place along a linear elastic line and not back down the loading curve. These effective strain and complementary strain energies cannot be obtained from the load–deflection curve as is assumed in the Ernst *et al.* (1981) scheme for calculation of J during propagation as we shall show.

One of us examined the problem of an elastic perfectly plastic cantilever glued to a massive block loaded at its end by a moment (Atkins & Mai 1986). In that case, because the end moment is constant during crack propagation and there is no unloading, the moment-rotation diagram for a real ELP material is identical to that for an NLE material. Hence in this case the effective strain and complementary strain energies can be obtained from the moment-rotation diagram for propagation as well as initiation. Williams (1993) also considered elastic perfectly plastic bending of beams in a review of energy release rates for strips in tension and bending.

During propagation the accumulated work, from which the plastic component of J_R is usually determined by the use of an η_p factor, is the sum of plastic work and the essential work. The J_R approach makes no attempt to distinguish between the essential work of fracture in the FPZ and the work dissipated in the plastic zone. While these two terms are usually coupled, in some situations the plastic work

can be altered independently of the essential work of fracture within the FPZ. For example in the quasi-mode III tearing of a strip from the edge of a ductile metal sheet the plastic work term relates to plastic bending and unbending of the strip and can be altered independently of the essential work of tearing within a narrow FPZ by altering the width of the strip torn off (Mai & Cotterell 1984). In this case it is obvious that J_R depends directly on the specimen size. Experimentally determined J_R curves can be predicted by embedding a FPZ†, which models the strain-softening behaviour with the Gurson model, in incremental plasticity finite element analyses. The values of the strain-hardening exponent and the initial void volume fraction, that give the best fit to one specimen geometry and size in these analyses, are used very successfully to predict the load–deflection and J_R curves for other geometries and specimen sizes (Xia *et al.* 1995; Xia & Shih 1995). Unfortunately there is no separation of the essential work of fracture from the plastic work of fracture in these analyses. However, the essential work of fracture can be obtained at initiation because $J_{Ic} \approx R$. The essential work of fracture, R, can vary in these analyses because the deformation within the FPZ is dependent on the constraint. However, as already argued, the deformation within the FPZ must be nearly one of uniaxial strain. Therefore the major influence of constraint occurs prior to the material entering the FPZ. Hence the essential work of fracture in the FPZ may not vary greatly with specimen geometry and size even though the constraint provided by the specimen can be very different.

The deeply side-grooved DCB geometry studied in this paper has been chosen because it eliminates many complications in ductile fracture and a closed-form solution is possible. The invariant nature of crack propagation and the deep side grooves, produce a straight fracture front without the complication of thumbnail-crack-front tunnelling and the build up of shear lips during propagation which can cause a real increase in the essential work of fracture. Hence crack propagation in the DCB specimen is nearly steady-state and it will be shown to take place at a constant value of the essential work of fracture, R.

2. A preliminary experiment

Figure 1 shows the load–deflection curves for two deeply side-grooved 6082-TF aluminium alloy DCB specimens (see table 1) having different initial fatigued crack lengths, but otherwise identical. This particular alloy's stress-strain behaviour approximates well to an elastic perfectly plastic solid. The specimen 1A with the shorter initial crack length was loaded until the crack had propagated to the same length as the initial crack length of the second specimen, 2A. Specimen 2A was then loaded up to initiation. In both specimens, the arms were partially plastic before a crack was initiated. The load–deflection (P–u) coordinates of the two specimens under load at the same crack length would be identical for a true NLE material. Figure 1 demonstrates that this is obviously not the case: the deflection under load of specimen 2A, which had an initial crack length of 70 mm, is only 14 mm, whereas the deflection of specimen 1A, which was propagated to a crack length of 140 mm from a 70 mm crack, is 25 mm. Furthermore, the unloaded deflections are very different (1 mm compared with 12 mm).

† It is simpler to embed a strip of Gurson material ahead of the crack tip, rather than attempt to define the length of the FPZ.

Table 1. *Material properties and dimensions of DCB specimens*

((a) Aluminium alloy 6082-TF (these were unequal arm specimens, with one arm elastic). Young's modulus, E, 68 GPa. Yield strength, σ_y, 291 MPa.)

specimen	height of elastic beam (mm)	height of plastic beam $2h$ (mm)	gross beam width $2b$ (mm)	net beam width $2b_n$ (mm)	initial crack length l_i (mm)
1A	12.7	8.6	4.92	1.11	70
2A	12.7	8.6	4.92	1.11	140
3A	12.5	7.95	4.92	1.11	101
4A	12.7	8.6	4.92	1.11	80
5A	12.7	8.6	4.92	1.11	142.5
6A	16.0	16.0	4.92	1.11	82.5

((b) α-brass. (These were equal arm specimens.) Young's modulus, E, 106 GPa. Yield strength, σ_y, 230 MPa. Strain hardening index, n, 0.33.)

	beam height $2h$ (mm)	gross beam specimen width $2b$ (mm)	net beam width $2b_n$ (mm)	initial crack length l_i (mm)
1B	6.0	6.37	0.4	90
2B	6.0	6.37	0.4	130
3B	24.5	6.37	0.4	170

The cause of the extra deflection is to be found in the different plastic zones in the arms of the two specimens. In figure 2*a*, BCDB and the corresponding zone below the neutral axis represent the plastic zone at crack initiation in the specimen with a 70 mm starter crack. The plastic deformation, as detected by strain gauges and estimated from the yield strength, extended some 20 mm back from the crack tip along the arms of the DCB specimen. Calculations show that the maximum depth of yielding CD to be 2.4 mm. When the crack has propagated to a total length of 140 mm, the plastic zone is given by BEFDB in figure 2*b*. In contrast the plastic zones at initiation in the second specimen, having a 140 mm initial crack, are given by GEFG, figure 2*c*, and extend some 40 mm back from the crack tip, but with the same maximum depth EF as in the first specimen. The depth of the plastic zone is the same in both cases because experiment shows that elastoplastic propagation in the DCB specimen occurs at constant crack tip moment, Pl. The irreversible deformation associated with the zone BGFDB is the origin of the greater deflection for the first specimen. In NLE, the deformation in the zone BGFDB is elastic and there is no locked-in residual elastic strain. All the energy is recoverable in NLE. However, in real ELP bodies such zones represent irreversible work and even the linear elastic strain energy cannot be fully recovered. Incorporation of the irreversibly deformed zones left behind the moving crack front is crucial for proper elastoplastic propagation analyses in this and other geometries. NLE, which is the basis of the J_R approach, cannot predict the experimental results shown in figure 1.

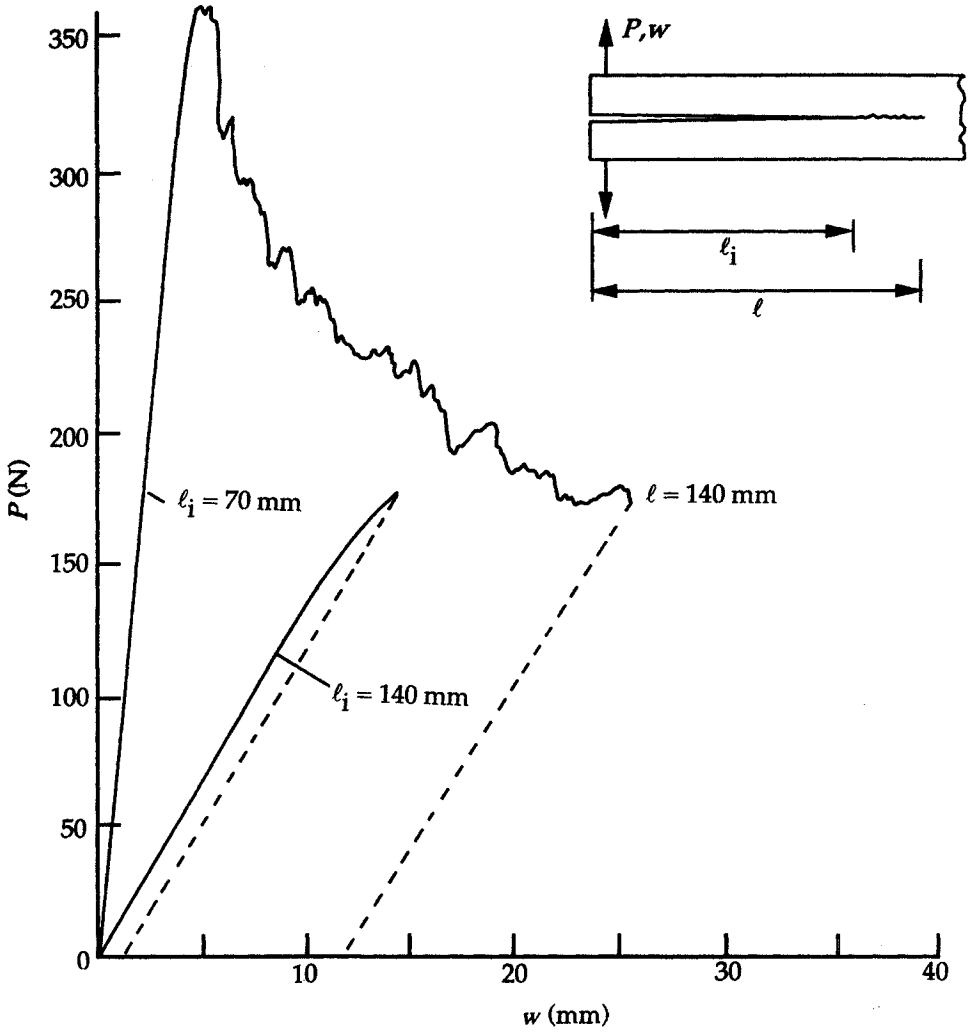

Figure 1. Load–deflection P–u curves for two elastoplastic DCB specimens 1A, 2A (6082-TF aluminium alloy) having different initial crack lengths, but otherwise identical, showing the ELP and NLE difference.

3. The post yield fracture mechanics of the DCB specimen

The fracture analysis of the related problem of an elastic perfectly plastic cantilever glued to a massive block was given by Chang *et al.* (1972). However, their solution cannot be applied to propagation, because they did not consider the residual zones of plasticity and non-recoverable elastic energy. Hence theirs is really an NLE solution.

All the equations are given for a symmetrical DCB specimen with equal arms. The modification to an asymmetrical DCB specimen is trivial and is not presented.

(*a*) *Fracture of an elastic perfectly plastic deeply side-grooved DCB specimen*

The DCB specimen can be analysed using the engineers' theory of bending. However, the deep side grooving introduces considerable compliance at the tip of the crack and deformation in the deeply side-grooved region has to be considered. The main effect of the increased compliance due to the side grooving will be elastic,

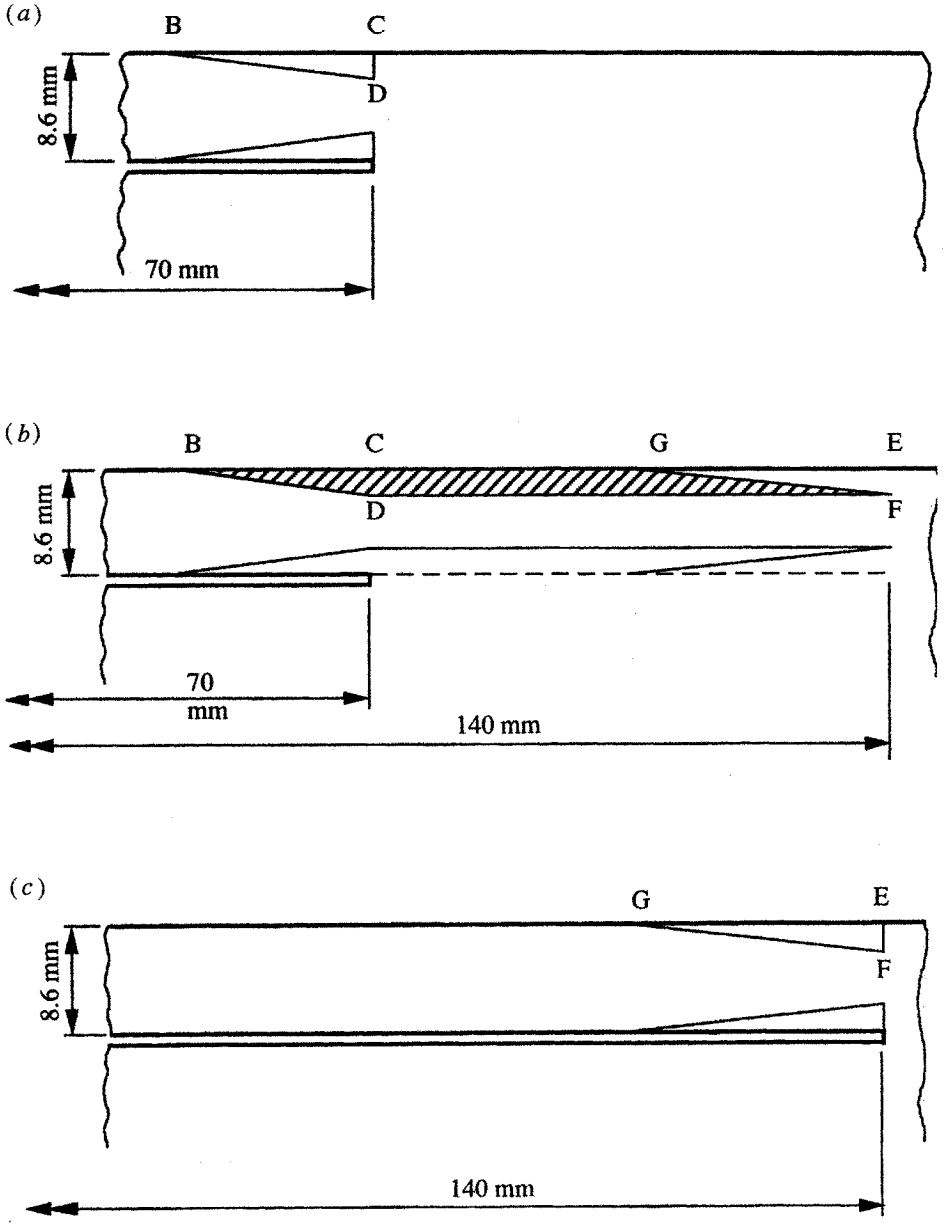

Figure 2. The different elastoplastic zones in the two cases of figure 1. (*a*) BCDB is the plastic zone at crack initiation for the 70 mm initial crack. (*b*) After propagation to 140 mm, plasticity extends over BCGEFDB. (*c*) GEFG is the plastic zone at crack initiation for the 140 mm initial crack.

though the cantilever beams will also actually yield slightly ahead of the crack tip and a fracture process zone will exist. Hence in this analysis a small elastic rotation and a very small deflection are allowed at the crack tip which is calculated from the theory of beams on elastic foundations (Timoshenko 1956). A fuller treatment of the effect of the deep side-grooving allowing for plastic deformation in the side-grooved section and the beam ahead of the crack tip has been given by Cotterell *et al.* (1996). Hence the load-line deflection at initiation, u_i, of an elastic perfectly plastic deeply

side-grooved DCB has been obtained from the expression of Chang *et al.* (1972) by the addition of a deflection due to the 'elastic foundation' and is given by

$$u_i = \frac{160}{27P^2E}\sigma_y^3 b^2 h^3 - \frac{4(4\sigma_y bh^2 + Pl)}{9P^2E}\sqrt{2\sigma_y^3 b(6\sigma_y bh^2 - 3Pl)} + \frac{3P[1 + 2(\beta l) + 2(\beta l)^2]}{4Ebh^3\beta^3}, \tag{3.1}$$

where E is the Young's modulus and the height and gross width of the beams are $2h$ and $2b$, respectively. If the side grooves are square sided with a height of $2h_n$ and width $2b_n$, the elastic foundation parameter can be approximated by

$$\beta = \left[\frac{3(1-\nu)}{8(1+\nu)(1-2\nu)bh^3}\left(\frac{b_n}{h_n}\right)\right]^{1/4}, \tag{3.2}$$

where ν is the Poisson's ratio, assuming that the stress within the grooved section is uniform across the width and height. However, because both square and vee-grooves were used in the experiments, the value of the β used in the analysis was experimentally determined from the elastic load-deflection using independent values for E and ν.

At the crack tip no unloading occurs even during propagation and hence the curvature at the crack tip, κ_1, can be written in terms of the crack tip bending moment, M_1, which is given by

$$M_1 = Pl = 2bE\left[\varepsilon_y h^2 - \frac{\varepsilon_y^3}{3\kappa_1^2}\right]. \tag{3.3}$$

The effective strain energy density (including plastic as well as elastic deformation) per unit length of the beam at the crack tip, λ_1, can be written in terms of the crack-tip beam curvature and is given by

$$\lambda_1 = 2Eb\left[\frac{\varepsilon_y^3}{3\kappa_1} + \varepsilon_y\kappa_1 h^2 - \varepsilon_y^2 h\right], \tag{3.4}$$

where ε_y is the uniaxial yield strain. Adding to this the small rate of change in elastic strain energy stored in the 'elastic foundation' and beam ahead of the crack tip, the partial derivative of the effective strain energy with respect to the crack area at constant load for the specimen is

$$\left[\frac{\partial \Lambda}{\partial A}\right]_P = 2E\frac{b}{b_n}\left[\frac{\varepsilon_y^3}{3\kappa_1} + \varepsilon_y\kappa_1 h^2 - \varepsilon_y^2 h\right] + \frac{3(Pl)^2(1+2\beta l)}{8Ebb_n h^3(\beta l)^2}. \tag{3.5}$$

Thus

$$\begin{aligned} J = R = \left[\frac{\partial \Omega}{\partial A}\right]_P &= \frac{Pl\kappa_1}{b_n} + \frac{3(Pl)^2(1+2\beta l)}{4Ebb_n h^3(\beta l)^2} - \left[\frac{\partial \Lambda}{\partial A}\right]_P \\ &= 2E\frac{b}{b_n}\left[\varepsilon_y^2 h - \frac{2\varepsilon_y^3}{3\kappa_1}\right] + \frac{3(Pl)^2(1+2\beta l)}{8Ebb_n h^3(\beta l)^2}. \end{aligned} \tag{3.6}$$

Equation (3.6) can be rewritten in terms of the full plastic moment M_p and the ratio $\xi = M_1/M_p$ as

$$R = \frac{2M_p^2}{3b_n EI}\left[1 - \frac{2}{\sqrt{3}}\sqrt{1-\xi} + \frac{3\xi^2(1+2\beta l)}{4(\beta l)^2}\right], \tag{3.7}$$

where I is the second moment of area of the beam. The first two terms in equation (3.7) are identical to an expression given by Williams (1993) who did not consider the possibility of rotation of the beam at the crack tip†.

Although the equilibrium load is the same for a crack of length l whether that is the initial crack length or the current crack length after some crack growth, the deflection is different as noted in the discussion of the preliminary results given in § 2. The deflection in the propagated crack is greater than that for a crack, of the same length, at initiation because of unrecovered accumulated plastic deformation. The curvature during unloading behind the crack tip is given by

$$\kappa = \kappa_{\mathrm{i}} - \frac{(M_{\mathrm{i}} - M)}{EI}, \tag{3.8}$$

where κ_{i} and M_{i} are the values of the curvature and the moment at crack initiation. There are three different deformation regions in the arms of the DCB specimen (see figure 3).

(1) That part of the beam which has always been elastic.

(2) That part of the beam from the elastic boundary to the tip of the initial crack.

(3) That part of the beam formed by the crack extension.

The curvature has to be integrated separately in these three regions. Thus the deflection, u, at the tip of the DCB specimen which has propagated at constant R from an initial crack length l_{i}, to a crack length l ($\Delta l = l - l_{\mathrm{i}}$), is given by

$$\begin{aligned} u = {} & \frac{160}{27}\frac{\sigma_{\mathrm{y}}^3 b^2 h^3}{P_{\mathrm{i}}^2 E} - \frac{4(4\sigma_{\mathrm{y}} b h^2 + P_{\mathrm{i}} l_{\mathrm{i}})}{9 P_{\mathrm{i}}^2 E}\sqrt{2\sigma_{\mathrm{y}}^3 b(6\sigma_{\mathrm{y}} b h^2 - 3P_{\mathrm{i}} l_{\mathrm{i}})} \\ & + \frac{3P}{4Ebh^3\beta^3}[1 + 2(\beta l) + 2(\beta l)^2] + \frac{l^2 - l_{\mathrm{i}}^2}{E}\sqrt{\frac{2\sigma_{\mathrm{y}}^3 b}{6\sigma_{\mathrm{y}} b h^2 - 3P_{\mathrm{i}} l_{\mathrm{i}}}} \\ & - \frac{(P_{\mathrm{i}} - P) l_{\mathrm{i}}^3}{2Ebh^3} + \frac{P\Delta l^3}{2Ebh^3} - \frac{3P\Delta l^2 l}{4Ebh^3}, \end{aligned} \tag{3.9}$$

where P_{i} is the load at initiation and P is the load after propagation to a crack length l. The first three terms of equation (3.9) are the NLE compliance. The rest of the terms are the history-dependent components of compliance in the elastoplastic case.

(*b*) *Fracture of an elastic power-law-hardening DCB specimen*

Similar expressions have been derived for a power-law hardening material defined by

$$\sigma = \begin{cases} E\varepsilon, & \text{for } \varepsilon \leqslant \varepsilon_{\mathrm{y}}, \\ \sigma_{\mathrm{y}}\left(\dfrac{\varepsilon}{\varepsilon_{\mathrm{y}}}\right)^n, & \text{for } \varepsilon \geqslant \varepsilon_{\mathrm{y}}. \end{cases} \tag{3.10}$$

A closed-form solution for the deflection is not possible because of the complex κ–M relationship and numerical solutions have been used. However, a closed form does exist for the essential work of fracture, R, for both initiation and propagation, which

† Williams's expression is for a single cantilever arm, but the two expressions look identical because we define b_{n} as half the width of the grooved section.

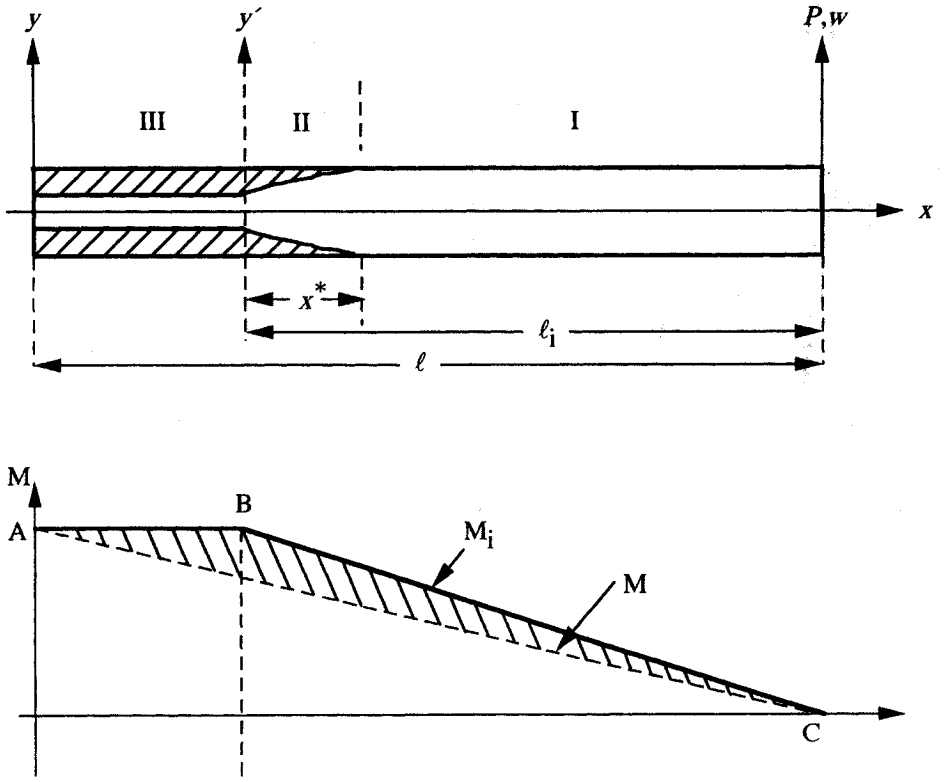

Figure 3. Unloading of an arm of a DCB specimen during equilibrium crack propagation and the three regions of deformation. During crack propagation from l_i to l the load decreases from P_i to P giving partial unloading of the cantilever arms. The height of the shaded are ABC represents the history of elastic unloading moments behind the crack tip.

can be obtained using the same method outlined in § 3 *a* and is given by

$$R = 4E\frac{b}{b_n}\left\{\frac{n\varepsilon_y\kappa_1 h^2}{(1+n)(2+n)}\left(\frac{\kappa_1 h}{\varepsilon_y}\right)^n + \frac{(1-n)h\varepsilon_y^2}{2(1+n)} - \frac{2(1-n)\varepsilon_y^3}{3(2+n)\kappa_1}\right\} + \frac{3(Pl)^2}{8Ebb_n h^3}\frac{(1+2\beta l)}{(\beta l)^2}. \tag{3.11}$$

(*c*) *The J_R curve and accumulated work*

For both initiation and propagation, there are schemes for calculation of the J integral from the area under the load–deflection curve for the standard fracture geometries such as compact tension and three-point bend (ASTM 1987). These schemes effectively ignore the real ELP nature of crack propagation and are the causes of spurious crack growth resistance because they include plastic work remote from the crack tip in J_R. The J integral in these schemes is obtained from equation (1.2) despite the fact that during crack propagation the effective strain energy is not obtainable from the load–deflection diagram.

For an NLE DCB specimen the load, P, can be expressed in terms of the displacement between the arms, u, by the functional form

$$P = \frac{2bh^2\sigma_y}{l}F\left(\frac{uh}{l^2}\right). \tag{3.12}$$

For initiation the J integral is given by equation (1.2) and is

$$J = -\left[\frac{\partial \Lambda}{\partial A}\right]_u = \frac{h^2 b \sigma_y}{b_n l^2} \int_0^u \left[F + \frac{2uh}{l^2} F'\right] \mathrm{d}u, \tag{3.13}$$

where F' indicates the derivative of F with respect to its argument. Integrating by parts one obtains

$$J = \frac{h^2 b \sigma_0}{b_n l^2}\left[2Fu - \int_0^u F\,\mathrm{d}u\right] = \frac{1}{2b_n l}\left[2Pu - \int_0^u P\,\mathrm{d}u\right]. \tag{3.14}$$

Splitting the displacement into elastic, u_e, and plastic, u_p, displacements, the J integral can be decomposed into an elastic component, J_e, which is equal to the energy release rate,

$$J_e = \frac{3(Pl)^2}{8Ebb_n h^3}\left[1 + \frac{(1+2\beta l)}{(\beta l)^2}\right], \tag{3.15}$$

and a plastic component J_p. Assuming rigid perfectly plastic deformation for the plastic deformation as in previous analyses of the notch bend (Rice *et al.* 1973) and compact tension geometries (Clarke & Landes 1979), the plastic component, J_p, for the DCB geometry at initiation can be written as

$$J_p = \frac{\eta_p}{2b_n l} \int_0^{u_p} P\,\mathrm{d}u_p, \tag{3.16}$$

where $\eta_p = 1$†. It will be seen in § 4 that J_{Ic} calculated from equations (3.15) and (3.16) agree with that given by equations (3.7) and (3.11) and we have no quarrel with this method. However, the difficulty arises when J_R is calculated making use of equation (3.16) because here the behaviour of an ELP and an NLE material are really quite different but they are treated as if they were the same.

Ernst *et al.* (1981) have derived a scheme for the calculation of J during crack propagation that applies to the compact tension and the three-point bend specimen. This method has been incorporated into the J_R standard ASTM E1152. For the DCB geometry, as in the analysis of Ernst *et al.* (1981), the elastic, J_e, and plastic, J_p, components are treated separately. The elastic component, J_e, during propagation is given by equation (3.15). Since the crack tip bending moment is practically constant during crack growth in the DCB specimen, the increment in the plastic component of the J integral, taking $\eta_p = 1$, can be rewritten as

$$\mathrm{d}J_p = \frac{Pl}{2b_n}\mathrm{d}\left(\frac{u_p}{l^2}\right). \tag{3.17}$$

Hence if at the rth increment $J_p = J_p^r$, then

$$J_p^{r+1} = J_p^r + \frac{Pl}{2b_n}\left[\left(\frac{u_p}{l^2}\right)_{r+1} - \left(\frac{u_p}{l^2}\right)_r\right]. \tag{3.18}$$

Equations (3.15), (3.16) and (3.18) have been used to construct J_R curves from our experimental DCB load–deflection records in the spirit of the method recommended by ASTM E1152.

† An alternative approximate analysis is to separate the plastic deflection from an elastic perfectly plastic DCB and to calculate η_p at the point of plastic collapse. In this case $\eta_p = 1.08$.

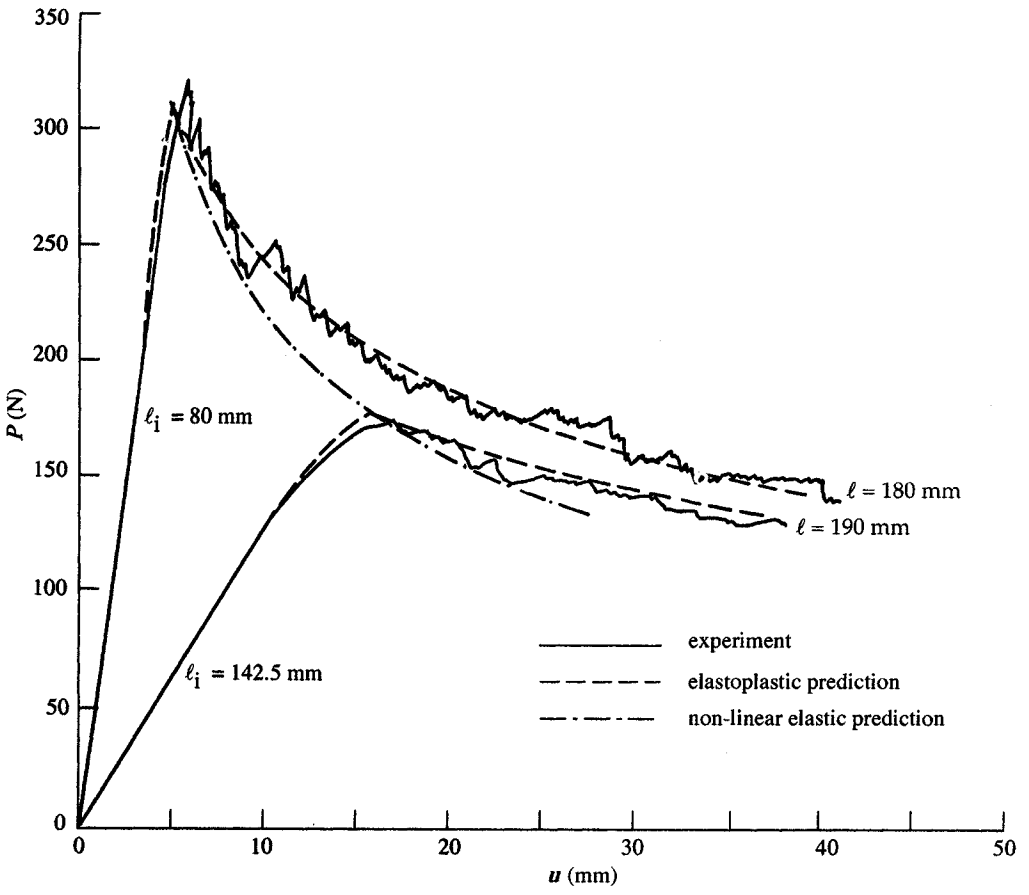

Figure 4. Load-deflection curves for two aluminium alloy DCB specimens, 4A and 5A, of the same beam height but different initial crack lengths.

4. Experiments and results

Two series of tests on deeply side-grooved DCB specimens have been made (see table 1). In the first series, A, the specimens were made from aluminum alloy 6082 TF which approximates to elastic perfectly plastic behaviour and in the second series, B, an α-brass with pronounced strain hardening was used. In each series different initial crack lengths and beam heights were employed. The brass specimens were symmetric (same height for each arm), but the aluminium alloy specimens were asymmetric in beam height, so that only one beam was elastoplastic during propagation. However, the elastic strain energy in the other beam was included in the energy balance. The initial cracks were all extended by fatigue at bending moments significantly below those necessary to cause yielding in the arms. In specimens 6A and 3B the beam heights were such that fracture took place under globally elastic conditions with no plasticity in either arm.

Figure 4 shows the P–u diagrams for the aluminium alloy specimens, 4A and 5A, which differed only in the initial crack lengths. As in the preliminary experiments described in § 2, it is clear that the P–u behaviour, at given propagated crack length, is path dependent. Figure 5 shows the behaviour of specimen 6A in which fracture

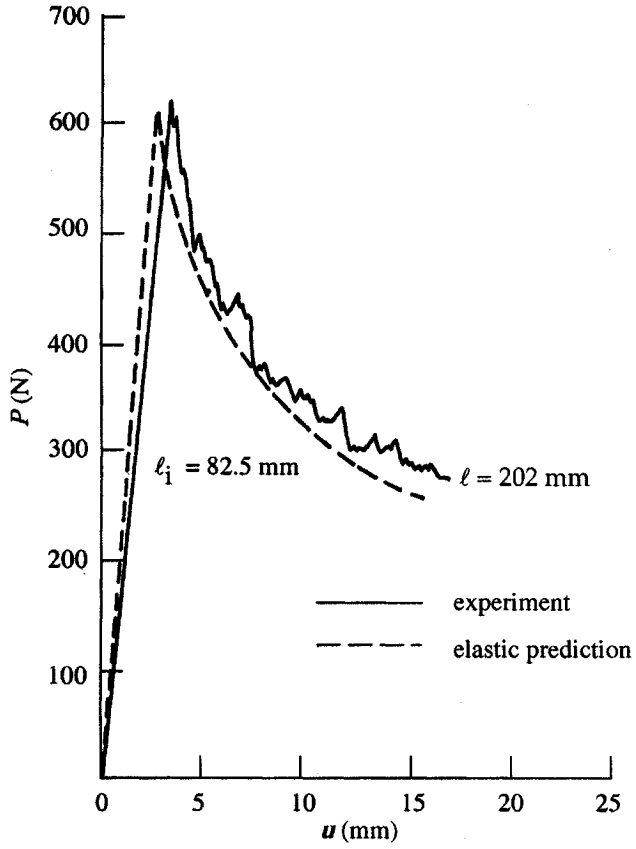

Figure 5. Load-deflection curve for an aluminium alloy DCB specimen, 6A, that is globally elastic.

was globally elastic. Figures 6 and 7 show the corresponding representative results for the α-brass.

Superimposed on the plots in figures 4–7 are the theoretical load–deflection plots for both initiation and propagation obtained from the analysis given in § 3, using the essential work, R, that gives the best fit. There is some underestimation of the deflection despite using a correction to allow for elastic deformation in the deeply side-grooved ligament, because the grooved section yields plastically before fracture†, but the elastoplastic fracture behaviour is largely reproduced. The effect of plastic stretching in the ligament can be seen in figure 7 for the globally elastic α-brass specimen, 3B, but is not evident in figure 5 for the globally elastic aluminum alloy specimen, 6A. Since the effective parameter, β, was obtained from the average elastic slope, the elastic slope predicted for specimen 6A is greater than observed.

The essential work of fracture, R, that gives the best fit is 25 kJ m^{-2} for the aluminium alloy and 75 kJ m^{-2} for the brass. It is once again clear that the curves for nonlinear elastic fracture mechanics (NLEFM) predictions, which are identical to elastoplastic initiation predictions, do not give the true P–u–l elastoplastic behaviour

† A treatment of a full solution allowing for plastic as well as elastic deformation in the deeply grooved ligament is given in Cotterell *et al.* (1996).

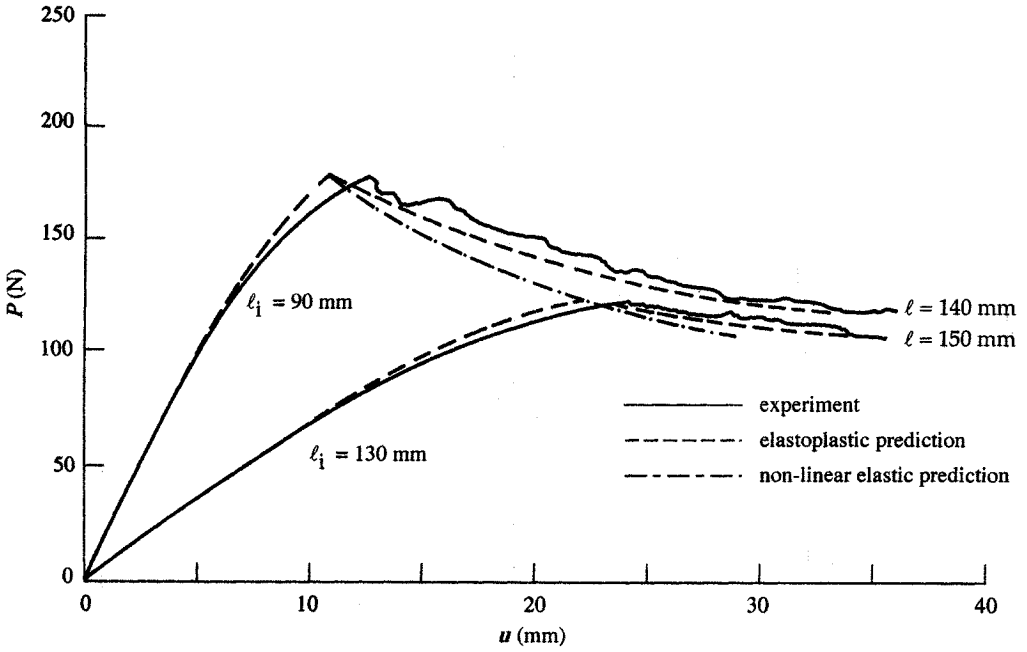

Figure 6. Load-deflection curves for two brass DCB specimens, 1B and 2B, of the same beam height but different initial crack lengths.

during propagation. However, the constant R loci predicted by NLEFM pass through the initiation coordinates.

The J_R curves presented in figures 8 and 9 for the aluminium and brass specimens have been obtained from the P–u curves using equations (3.15), (3.16), and (3.18). The initiation value, J_{Ic}, for the two materials are close to the estimated values of the essential works of fracture, R. There is no increase in J_R for series A specimens and little for series B specimens that are globally elastic, as is expected because here the NLE theory is exact and $J = R$. Since the increase in J_R comes from plastic work performed in deforming the arms, the beams of smallest height show the most increase. The J_R curves for beams of the same height, but with different initial crack lengths, are very similar as is predicted since the crack propagation is very close to steady-state. Superimposed on figures 8 and 9 are the J_R curves predicted from the theoretical P–u–l curves. There is excellent agreement with all the J_R curves except for specimen 3A where the theoretical J_R curve overestimates the experimental one.

5. Discussion and conclusions

It has been shown that because plastic deformation in the DCB specimen occurs under constant stress and strain ratios, the essential work of fracture, R, can be separated from the remote plastic work during crack propagation as well as at initiation. The energetic expression for J (equation (1.2)) holds for both initiation and propagation, if the effective strain and complementary strain energies for a DCB specimen that account for real unloading of an ELP material are used.

The results in figures 4 and 6 show that the loads and displacements at crack initiation in beams with different initial crack lengths all lie on the constant-R NLEFM locus. However, the results also make it clear that an NLEFM approach for ductile

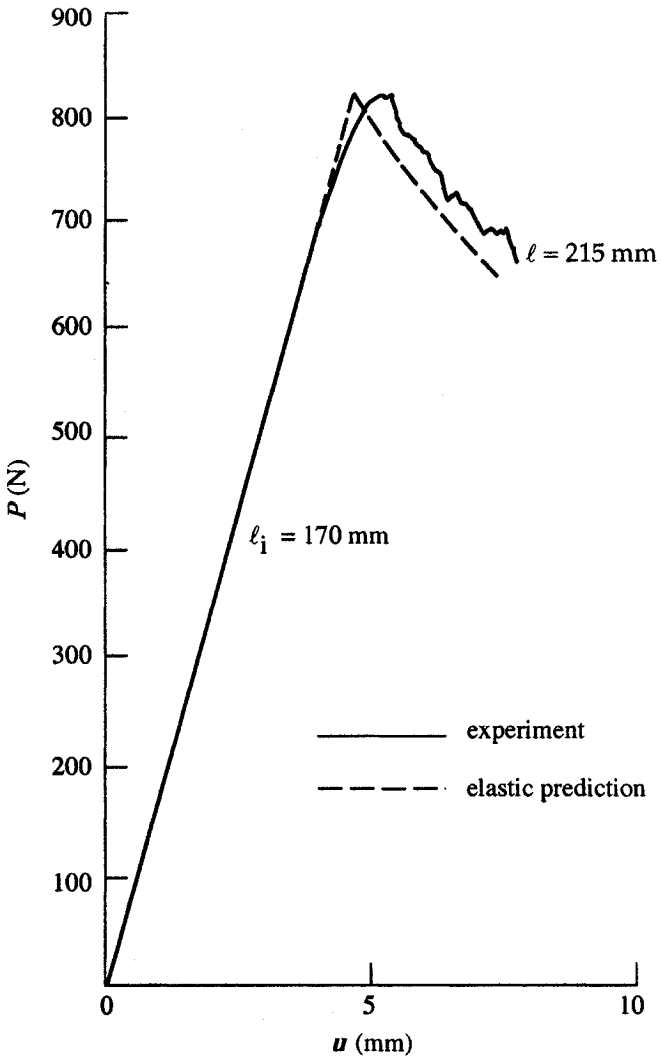

Figure 7. Load-deflection curve for a brass DCB specimen, 3B, that is globally elastic.

crack propagation is inappropriate. During propagation the path-dependent additional load-point displacements produced by the residual plastic zones left behind the crack and the associated unrecovered energies, invalidate NLEFM methods in practical elastoplastic fracture. The analysis given in this paper takes account of these factors, and our experiments show that the theoretical model well describes the results. Furthermore, it is important to note that our experiments show the propagation in a DCB specimen to occur at the same constant value of R during elastoplastic fracture as during displacement-reversible elastic fracture. In other words, the resistance to cracking is controlled throughout by the essential work of fracture. In other geometries where steady-state crack propagation is not possible, there can be a variation in the essential work of fracture, R, because there is either a development of real fracture resistance with crack growth, such as caused by the formation of shear lips (Krafft *et al.* 1961) or the size of the fracture process zone changes significantly (Cotterell & Atkins 1996).

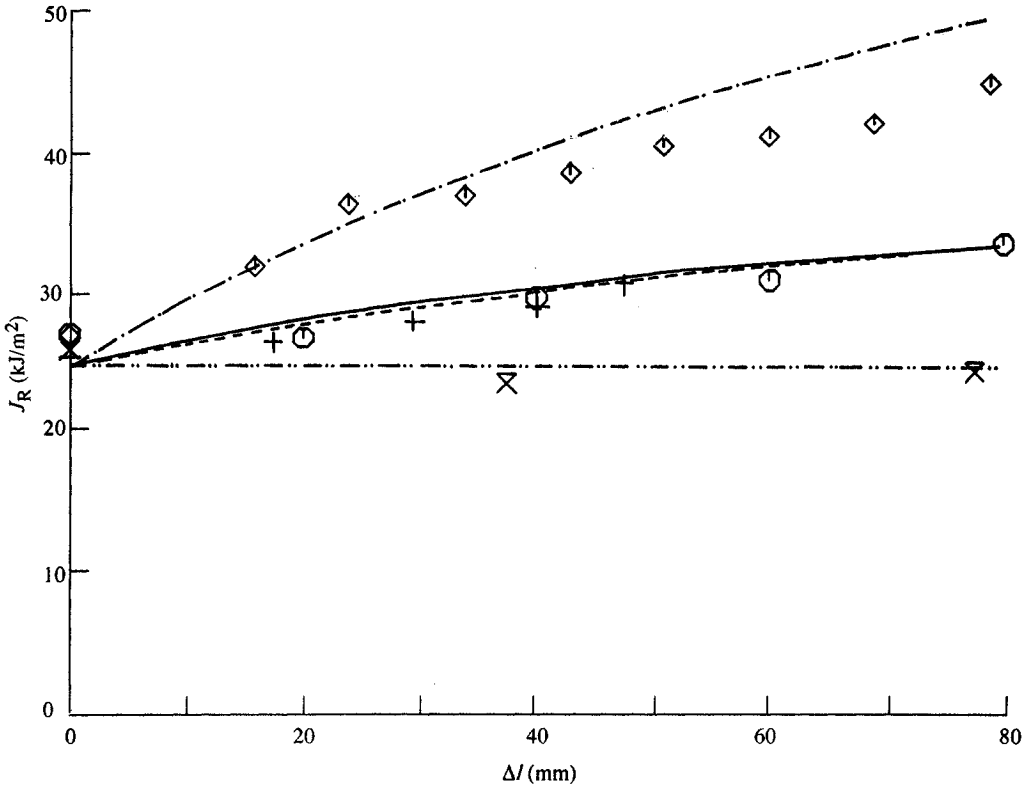

Figure 8. J_R curves for the aluminium alloy DCB specimens.

Fracture in the DCB specimen with deep side grooves does not meet an increase in resistance with crack extension. We have clearly shown that the essential work of fracture, R, is constant whether the arms of the DCB specimen remain elastic or suffer considerable plastic deformation. However, the J_R curves obtained from the load–deflection diagrams in the conventional manner show an increase with crack extension. Only the globally elastic specimens display a constant J_R. The increase in J_R depends on the height of the beams in the DCB specimen and becomes more pronounced as the height gets smaller. This conclusion is similar to the inferences in the work of Shih and his co-workers (Xia & Shih 1995; Xia *et al.* 1995) who by modelling the behaviour of the FPZ obtain J_R curves that show a larger increase with crack growth as the size decreases. The increase in J_R does not represent a real increase in toughness but is the result of using the load–deflection curve that contains a permanent plastic and locked-in residual elastic deformation. Since J_R contains plastic work from outside the fracture process zone as well as the essential work of fracture, R, performed in the fracture process, it cannot be used to predict fracture in any other geometry unless the two work components are separated. For side-grooved DCB specimen we have shown that the material size-independent term is the essential work of fracture, R. For other geometries, R may be somewhat dependent on crack growth and particular geometry, but the dependence is unlikely to be nearly as great as for J_R.

The deeply side-grooved DCB specimen examined in this paper is a highly special geometry and it is not the intention of the authors to suggest that such a specimen should be considered for a standard fracture test. However, what we have demon-

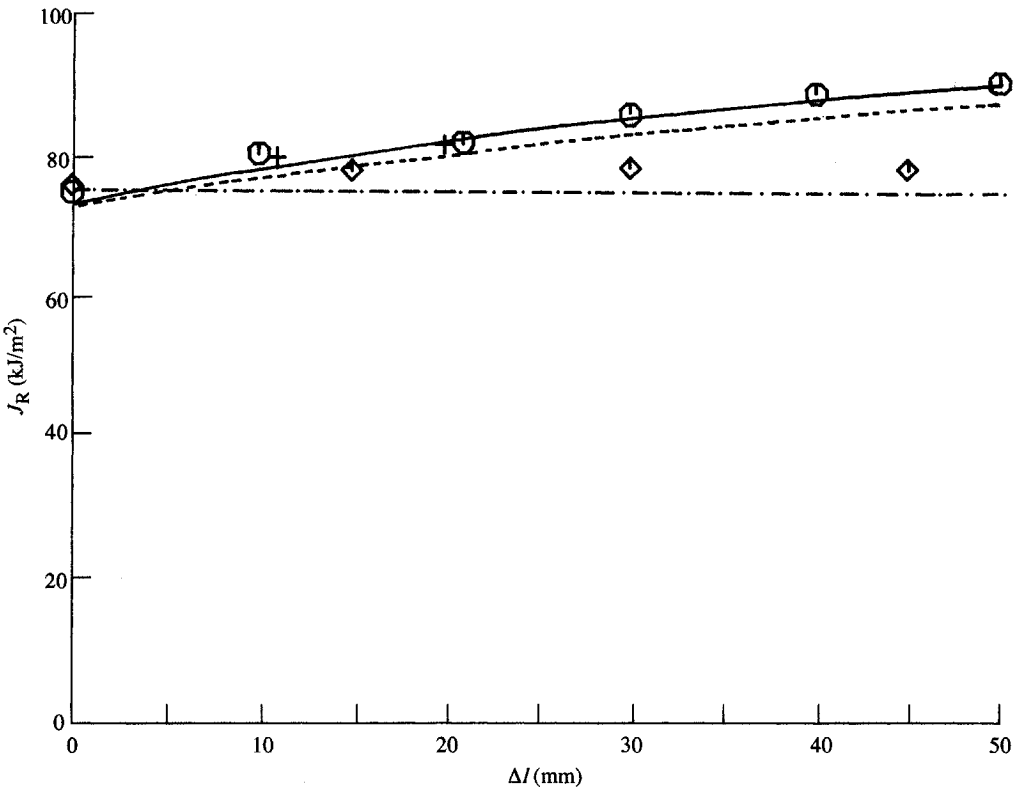

Figure 9. J_R curves for the brass DCB specimens.

strated is that the fundamental elastoplastic fracture parameter is the essential work of fracture, R. At initiation the J integral is identical to R. In general, J ceases to have a theoretical basis during propagation because it is only strictly applies to NLE materials but, because of the special nature of the DCB specimen, the energy expression for J is valid for propagation as well as initiation if the effective strain and complementary strain energies are correctly calculated. We have shown that J calculated from the load–deflection diagram after the manner of Ernst *et al.* (1981) is fallacious and gives a J_R that increases with crack extension, because it includes remote plastic work from outside the FPZ. The amount of plastic work depends upon the geometry, making J_R as calculated according to the ASTM E1152 unsuitable as a fracture parameter for crack propagation to enable the critical load to be determined for a structure. The essential work of fracture, R, which is not necessarily a constant, is a fundamental fracture parameter and it behoves the fracture community to seek suitable fracture tests for its measurement and to devise methods that can utilize it in design. One possibility that may give the essential work of fracture approximately for all geometries, is to construct an effective NLE load–deflection diagram by subtracting from the deflection the accumulated residual deformation which increases with crack extension which could perhaps be obtained from NLE empirical expressions similar to those used by Orange (1990). The Ernst *et al.* (1981) scheme for calculating J could then be used on this effective NLE load–deflection diagram and give a value of J that would not include remote plastic work and give the essential work of fracture, R. This method is not exact, but may be less objectionable than the present conventional method for calculating J_R curves and a way forward.

Support for this work from the European Economic Community under Contract CI1*-CT93-0327 is gratefully acknowledged. Thanks are also owed to the Chinese Government for a visiting Scholarship which enabled one of us to study at Reading. Alcan International's R&D Laboratories at Banbury kindly supplied the aluminium alloy plate from which the specimens were manufactured. Fruitful discussions were held with Professor E. Smith, for which we are grateful, and we thank Professor J. G. Williams and Professor K. Kendall for encouragement in getting this paper published. Finally, we pay tribute to Professor Charles Gurney, who died after this paper was written. His energy-based line of attack to fracture mechanics provided a foundation upon which we were able to build.

References

Atkins, A. G. & Mai, Y. W. 1986 *Int. J. Fract.* **30**, 203.

ASTM E 1152–87, 1987 Standard test method for determining J_R curves.

Chang, M. D., Devries, K. L. & Williams, M. L. 1972 *J. Adhesion* **4**, 221.

Clarke, G. A. & Landes J. D. 1979 *J. Testing Eval.* **7**, 264.

Cotterell, B. & Atkins, A. G. 1996 *Int. J. Fract.* **81**, 357.

Cotterell, B., Lam, K. Y., Chen, Z. & Atkins, A. G. 1996 In *Proc. IUTAM Symp. on nonlinear analysis of fracture, Cambridge* (ed. J. R. Willis), p. 105. Dordrecht: Kluwer.

Ernst, H. A., Paris, P. C. & Landes, J. D. 1981 In *Fracture mechanics. Proc. 13th National Symp., ASTM 743* (ed. R. Roberts), p. 476. Philadelphia, PA: American Society for Testing and Materials.

Griffith, A. A. 1921 *Phil. Trans. R. Soc. Lond.* A **221**, 163.

Gurson, A. L. 1977 *J. Engng Mater. Technol.* **99**, 2.

Hancock, J. W., Reuter, W. G. & Parks, D. M. 1993 In *Constraint effects in fracture, ASTM STP 1171* (ed. E. M. Hackett, K. H. Schwalbe & R. H. Dobbs), p. 21. Philadelphia, PA: American Society for Testing and Materials,

Havner, K. S. & Glassco, J. B. 1966 *Int. J. Fract. Mech.* **2**, 506.

Hutchinson, J. W. & Paris, P. C. 1979 In *Elastic-plastic fracture, ASTM STP 668* (ed. J. D. Landes, J. A. Begley & G. A. Clarke), 37. Philadelphia, PA: American Society for Testing and Materials.

Joyce, J. A. & Link, R. E. 1995 In *Fracture mechanics: 26th Symp., ASTM STP 1256* (ed. W. G. Reuter, J. H. Underwood & J. C. Newman), p.142. Philadephia, PA: American Society for Testing and Materials.

Kachanov, L. M. 1971 *Foundations of the theory of plasticity.* Amsterdam: North-Holland.

Krafft, J. M., Sullivan, A. M. & Boyle, R. W. 1961 *Symp. on Crack Propagation*, vol. 1, p. 8. Cranfield: College of Aeronautics.

Orange, T. W. 1990 In *Fracture mechanics: 21st Symp., ASTM STP 1074.*

Rice, J. R. 1968 In *Fracture* (ed. H. Liebowitz), vol. 2, p. 192. New York: Academic.

Rice, J. R., Paris, P. C. & Merkel, J. G. 1973 In *Progress in flaw growth and fracture toughness testing, ASTM STP 536*, p. 231. Philadephia, PA: American Society for Testing and Materials.

Timoshenko, S. 1956 *Strength of materials*, part II, 3rd edn. Princeton, NJ: Van Nostrand.

Tvergaard, V. 1982 *Int. J. Fract.* **18**, 265.

Williams, J. G. 1993 *J. Strain Analysis* **28**, 237.

Xia, L. & Shih, C. F. 1995 *J. Mech. Phys. Solids* **43**, 233.

Xia, L., Shih, C. F. & Hutchinson, J. W. 1995 *J. Mech. Phys. Solids* **43**, 389.